PHYSICAL REVIEW E **70**, 050101(R) (2004)

Tractable theory of nonlinear response and multidimensional nonlinear spectroscopy

Russell DeVane, Christina Ridley, and Brian Space*
Department of Chemistry, University of South Florida, 4202 E. Fowler Avenue, SCA400, Tampa, Florida 33620-5250, USA

T. Keyes
Department of Chemistry, Boston University, Boston, Massachusetts 02215, USA
(Received 4 May 2004; published 16 November 2004)

Nonlinear spectroscopy provides insights into dynamics, but the response functions required for its interpretation pose a challenge to theorists. We proposed an approach in which the fifth-order response function $[R^{(5)}(t_1,t_2)]$ was expressed as a two-time classical time correlation function (TCF). Here, we present TCF theory results for $R^{(5)}(t_1,t_2)$ in liquid xenon. Using a first-order dipole-induced dipole polarizability model, the result is compared to an exact numerical calculation showing remarkable agreement. In addition, $R^{(5)}(t_1,t_2)$ is calculated using the exactly solved polarizability model, yielding different results and predicting an echo signal.

DOI: 10.1103/PhysRevE.70.050101 PACS number(s): 82.53.Uv, 78.47.+p

Multidimensional nonlinear spectroscopic techniques are emerging as powerful tools that can reveal the microscopic structure and dynamics of condensed phases and biomolecules on ultrafast (subpicosecond) time scales. For example, they offer the possibility of differentiating between homogeneous and inhomogeneous broadening processes, which is difficult with traditional spectroscopy [1]. The fifth-order, two-dimensional (2D) Raman spectrum, which has been the subject of many recent experimental [2–6] and theoretical [7–14] investigations, is well suited to the study of low frequency, intermolecular, motions in liquids. The circumvention of previous difficulties by using heterodyne detection has reinforced interest in the 2D Raman experiment [2–6]. The 2D Raman spectrum also was predicted to show an echo feature along the diagonal time slice if intermolecular modes were sufficiently long lived although no echo has been found to date.

Multidimensional spectroscopy cannot achieve its full potential until an unambiguous theoretical framework is available; this presents a considerable theoretical challenge. An *n*-dimensional spectrum is given by an *n*-dimensional response function, a quantum average of nested commutators of *n* Heisenberg representation variables at different times. Even the classical limit yields quantities that are far more complex than familiar time correlation functions (TCF). In fact, it has been demonstrated that nonlinear spectra cannot be expressed exactly in terms of TCF [15].

Nevertheless, we recently proposed an approximate TCF theory of nonlinear spectroscopy that is computationally tractable for complex molecular condensed phase systems and is capable of accurately describing both intermolecular and intramolecular vibrational spectra. TCF theories are desirable because they allow nonlinear spectra to be calculated for realistic molecular dynamics (MD) models of condensed phase systems. It is essential that the theory be tested in a unambiguous manner. Previously we have presented explicit calculations of the 2D Raman spectrum of liquid CS_2, determined by the fifth-order response, $R^{(5)}(t_1,t_2)$ [16]. The 2D Raman spectra were in excellent agreement with extant experiments and approximate theoretical results [2,9,17]. But the agreement does not represent a rigorous test because uncertainties still exist in the experimental measurements and the theoretical results use approximate methods and different molecular models. Using the TCF theory, here we present the 2D Raman spectrum for liquid xenon using both first-order dipole-induced dipole (FODID) and exact [many body polarizability (MBP)] solutions of the dipole-induced dipole polarizability model. Ma and Stratt [12] carried out a numerically exact simulation of the fully polarized, $R^{(5)}_{xxxxxx}(t_1,t_2)$, 2D Raman spectrum of liquid Xe using the FODID model. Exact calculations can be performed for simple, small systems [9,12,17] only because of the computational burden. In this paper it is demonstrated that the TCF theory of $R^{(5)}\times(t_1,t_2)$ quantitatively reproduces the Ma-Stratt simulation, providing support for its further applications to more complex systems; TCF calculations with more extensive molecular models are not computationally difficult [16]. Further, the theory predicts a very different spectrum using the MBP model, including a significant echo feature for the $R^{(5)}_{xxzzxx}\times(t_1,t_2)$ polarization condition that was earlier suggested to be likely to emphasize an echo signature [18]. This echo occurs with a period that corresponds to frequencies in the heart of the xenon vibrational density of states (DOS), implying the existence of intermolecular vibrational modes that last for at least one full period [12].

The TCF theory describes the nonlinear response in terms of fully anharmonic MD calculations that are supplemented by a suitable spectroscopic (dipole and polarizability) model. Thus, it is demonstrated here, that while exact TCF expressions for nonlinear spectroscopy are not possible, effective TCF theories can be constructed. Such theories are powerful because they can be evaluated using atomistically detailed MD on complex liquids and solutions. TCF theories have distinct advantages over alternative approaches because they eliminate the need for costly classical calculations that are

*Author to whom correspondence should be addressed.

 ©2004 The American Physical Society

limited to small systems and intermolecular dynamics [9,12,17] and quantum calculations that rely on low-dimensional model systems [19]. It then becomes possible to predict and interpret nonlinear spectra for a wide variety of chemically important systems. In addition to its computational tractability, the TCF theory also makes a more manageable starting point for the development of theories based on the fifth-order response function.

The development of the TCF theory of $R^{(5)}(t_1,t_2)$ will be briefly revisited here; details are provided in our earlier work [16]. First consider the quantum mechanical expression for the electronically nonresonant fifth-order polarization response [13,17]: $R^{(5)}_{\alpha,\beta,\gamma,\delta,\epsilon,\phi}(t_1,t_2)=(i/\hbar)^2\mathrm{Tr}\{\Pi^{\alpha\beta}(t_1+t_2)\times[\Pi^{\gamma\delta}(t_1),[\Pi^{\epsilon\phi}(0),\rho]]\}$. In this equation, $\rho=e^{-\beta H}/Q$ for a system with Hamiltonian H and partition function Q at reciprocal temperature $\beta=1/kT$, and k is Boltzmann's constant; Tr represents a trace, square brackets denote commutators, Π is the system polarizability tensor, and the greek superscripts denote the elements and thus the polarization condition being considered. The classical limit of the trace is of order $\hbar^2$ and results from a combination of four two-time correlation functions that are themselves equivalent classically.

Expanding the commutators in the above equation gives $R^{(5)}(t_1,t_2)=(-1/\hbar^2)[g(t_1,t_2)-f^*(t_1,t_2)-f(t_1,t_2)+g^*(t_1,t_2)]$. Here, $f(t_1,t_2)=\langle\Pi^*(t_1)\Pi(t_2)\Pi\rangle$, $g(t_1,t_2)=\langle\Pi(t_2)\Pi\,\Pi^*(t_1)\rangle$, $f^*(t_1,t_2)=\langle\Pi\,\Pi(t_2)\Pi^*(t_1)\rangle$, and $g^*(t_1,t_2)=\langle\Pi^*(t_1)\Pi\,\Pi(t_2)\rangle$; an asterisk denotes the complex conjugate. The superscript notation on Π is now suppressed and the results apply to all possible polarizations. The angle brackets represent an equilibrium average. The expression inside the square brackets is the difference between the real part of the functions g and f, $g_R(t_1,t_2)-f_R(t_1,t_2)$, that must be of order $\hbar^2$ in the classical limit. It is easy to show that a multiplicative factor of leading order $\hbar$ can be obtained exactly using frequency domain (detailed balance) relationships between g and f, e.g., $e^{\beta\hbar\omega_1}g(\omega_1,\omega_2)=f(\omega_1,\omega_2)$; the frequency domain functions are the Fourier transform of the time domain functions. A sum of real and imaginary parts of a single two-time TCF then remains, and their $O(\hbar)$ contribution is required for the classical limit to exist in the form of a TCF.

For a one-time correlation function, $C(t)$, a simple frequency domain relationship exists between the real and imaginary parts, $C_I(\omega)=\tanh(\beta\hbar\omega/2)C_R(\omega)$ [20]. If a similar relationship between the real and imaginary parts of the two-time correlation function existed the fifth-order response could be written as second derivatives in time of a classical TCF, but no exact analytic relationship is possible and, therefore, an exact TCF theory is also not possible. However, an approximate relationship between the real and imaginary parts of the quantum TCF can be found for a harmonic system with the polarizability expanded to second order in the harmonic coordinate, Q, $\Pi=\Pi^0+\Pi' Q+1/2\Pi'' Q^2$. The real and imaginary parts are related as $g_I(\omega_1,\omega_2)=\tanh[-\beta\hbar(\omega_1/4+\omega_2/2)]g_R(\omega_1,\omega_2)$, where the subscripts denote the Fourier transform of the real or imaginary parts of the TCF's, both of which are real functions of frequency. This harmonic "reference" system is the simplest one that produces a fifth-order response and represents the leading contributions to the spectroscopy, analogous to IR intensities being given by the squared dipole derivative for a mode of a harmonic system with a linearly varying dipole [8,21]. The result is not a harmonic theory—fully anharmonic dynamics are used to calculate the relevant TCF—the approximation only serves to weight the different phonon processes implicit in the anharmonic MD as they would contribute in the harmonic system [8].

Using this relationship, the exact quantum mechanical response function can be written in terms of a classical TCF. The fifth-order response function, in the classical limit $\hbar\omega \ll kT$, takes the form $R^{(5)}(t_1,t_2)=-\beta^2/2[\partial^2 g_R(t_1,t_2)/\partial t_1^2-2\partial^2 g_R(t_1,t_2)/\partial t_1\partial t_2]$, and $g_R(t_1,t_2)\to\langle\Delta\Pi(0)\Delta\Pi(t_1)\Delta\Pi(t_1+t_2)\rangle$, the classical two-time TCF. Here, $\Delta\Pi=\Pi-\langle\Pi\rangle$ and the TCF is written in terms of the correlated polarizability fluctuations [16]. This represents our TCF theory of $R^{(5)}$. The expression is the classical limit of a more general result which, in the case of intramolecular spectroscopy, can be evaluated for high frequencies if one approximates the quantum mechanical TCF with the (quantum corrected) classical TCF. Because fifth-order Raman spectroscopy has primarily been applied to intermolecular dynamics, only the classical limit will be considered here.

$R^{(5)}(t_1,t_2)$ can be evaluated using MD and a model of the systems polarizability. It exhibits the correct limiting behaviors, including giving zero signal at the origin and everywhere along $t_2=0$. Also, the two-dimensional spectrum for ambient CS_2, calculated using our theory, was shown to be in excellent agreement with existing experimental and theoretical work [3,9,16].

The most rigorous test of this theory is to compare the resulting spectra to those from exact numerical results for the same model system. To evaluate this approach exactly, the classical limit is taken directly by replacing the commutators with Poisson brackets. Then, $R^{(5)}$ is seen to contain brackets of variables at different times, which requires the exceedingly difficult task of calculating the dependence of a many-body dynamical variable on its initial conditions. Calculating $R^{(5)}$ in this way is only practical for small simple systems and results for liquid xenon were reported previously [12]. To compare our theory to those results, microcanonical MD simulations were performed for the neat liquid xenon consisting of 108 atoms. The atoms interacted via a Lennard-Jones pair potential and the systems reduced density and temperature were $\rho\sigma^3=0.8$ and $kT/\epsilon=1.0$ and the same model parameters were used as in the exact calculation [12].

Results for the square of the fully polarized fifth-order response function, $|R^{(5)}_{xxxxxx}(t_1,t_2)|^2$, within the FODID approximation, are shown in Fig. 1. The result using our TCF theory is overlayed on the exact classical calculation performed by Ma and Stratt [12]; even though an exact TCF theory is not possible [15], the present theory is very effective. It captures the characteristic features present in the exact calculation, including the same decay times and the lack of an echo signal along the diagonal—which implies that the intermolecular modes have lifetimes of less than a full period. The signal is sharply peaked around $t_1\approx 30$ fs, $t_2\approx 350$ fs. Decay times vary along each axis with the signal

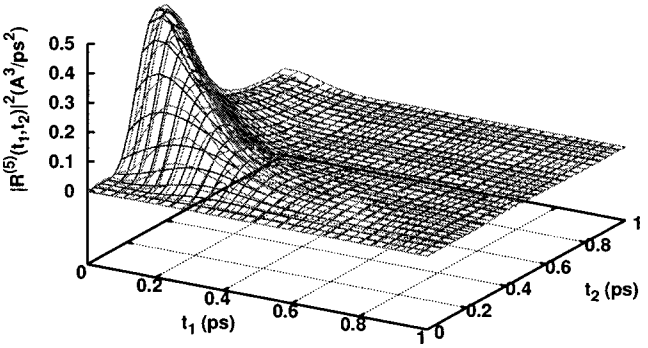

FIG. 1. Results for $|R^{(5)}_{xxxxxx}(t_1,t_2)|^2$ using the FODID approximation for liquid xenon. The exact classical molecular dynamics calculation (red, dark), Stratt *et al.* was reported in arbitrary units and is normalized here to our TCF theory data (green, light) at the maximum point.

dying out along t_1 by 400 fs; along t_2 there is a long time decay that continues beyond the 1 ps that is shown. In contrast to liquid xenon, the plot of the spectrum of CS_2 [2,16] is roughly symmetric, so the extreme asymmetry of the xenon simulation, with the peak practically on the t_2 axis, is striking [2,9,16]. The capability of the TCF theory to correctly yield symmetric or asymmetric spectra is further strong evidence of its general applicability.

To highlight the effectiveness of the TCF theory, Fig. 2 shows a slice of $|R^{(5)}_{xxxxxx}(t_1,t_2)|^2$ along t_2 with $t_1=0$. The dashed line is from the exact classical calculation and the solid line marked with squares represents the same result shifted forward in time by 34.7 fs. The solid line without symbols is from our TCF theory. The TCF result and the time-shifted exact calculation show quantitative agreement. The difference between the exact result and the TCF theory, the shift in time, is very likely due to finite system size effects on the exact calculation. Ma and Stratt were limited to using only 32 atoms in their simulation—even within the

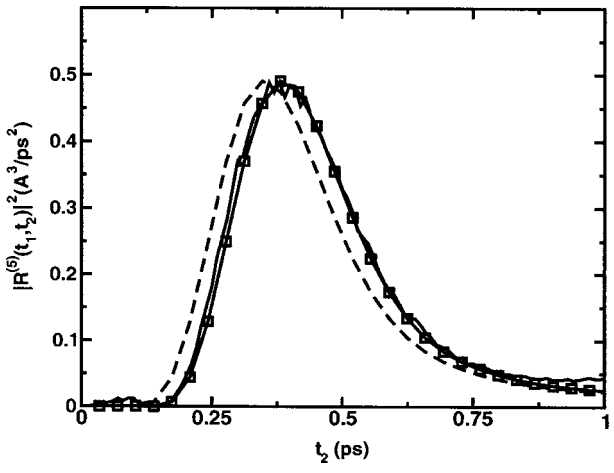

FIG. 2. Slices of $|R^{(5)}_{xxxxxx}(t_1,t_2)|^2$ along t_2 with $t_1=0$. The dashed line represents the exact classical calculation, the line marked with squares represents the time-shifted exact classical calculation, and the solid line without symbols represents the result from the TCF theory.

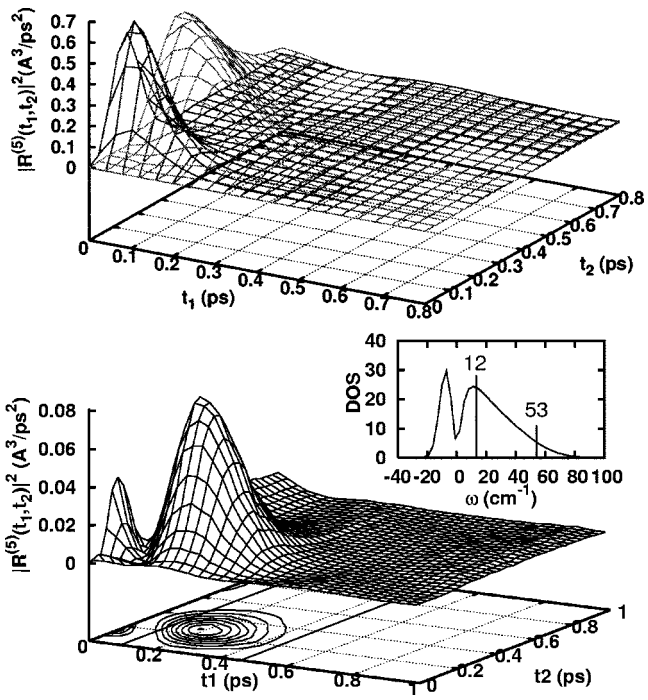

FIG. 3. The upper panel compares the TCF theory results for $|R^{(5)}_{xxxxxx}(t_1,t_2)|^2$ using the MBP model (red, dark, peaks earlier) vs the FODID approximation (green, light). The lower panel shows $|R^{(5)}_{xxzzxx}(t_1,t_2)|^2$ for liquid xenon using the MBP model. The solid lines parallel to the t_2 axis represent the width and location of (the beginning and end of) the echo peak along the diagonal (0.1 ps, 0.45 ps)—using the diagonal to choose the lines leads to them overlapping off-diagonal features in the figure. The inset shows the INM DOS for liquid xenon with vertical lines placed to show the breath of the vibrational periods associated with the echo peak.

FODID approximation that is far less computationally demanding than a MBP evaluation of the polarizability. To test the effect of the small system size they performed a simpler calculation of a one-dimensional slice of $\partial^2 g_R(t_1,t_2)/\partial t_1 \partial t_2|_{t_2=0}$ for 32 and 108 atoms because a non-Poisson bracket piece of the fifth-order signal with this form may be identified [14]. The resulting line shape had the same shape but with a time phase shift nearly identical to that apparent in Fig. 2 (see Fig. 4 of their paper), implying that the present theory may agree even better then the figure suggests [12].

Figure 3 shows $|R^{(5)}(t_1,t_2)|^2$ for liquid xenon using the MBP model. The MBP result is a prediction of the experimental fifth-order response function—xenon is highly polarizable and the FODID approximation is not strictly valid. The use of the FODID model effectively acts to remove contributions from the trace of the polarizability matrix [12]—one of three matrix invariants (in isotropic media) that give rise, in different combinations, to the signals for different polarization conditions [18]. Although the trace contributions are small in 1D correlation functions [12], in 2D correlation functions the invariants appear as products and a zero trace invariant kills off other significant terms that include sizable invariants multiplied by the trace contribution [18]. Thus, the use of the FODID approximation in the 2D correlation func-

tions acts to remove significant contributions that lead to different signals—including removing the echo contribution.

The upper panel of Fig. 3 compares results for $|R^{(5)}_{xxxxxx}(t_1,t_2)|^2$ using the MBP model (red) and the FODID model (green). The most notable differences are that the MBP signal has faster decay times, along both the t_1 and t_2 axis, and the peak is shifted to earlier times along t_2. The signal is characterized by a strong peak around $t_1 \approx 45$ fs, $t_2 \approx 125$ fs and dies out by 200 fs along both t_1 and t_2. As in the FODID approximation, no echo signal appears along the diagonal and the signal appears featureless beyond 300 fs in both t_1 and t_2 directions. While the FODID model captures much of the response, the distinct differences observed are a result of the exclusion of the polarizability tensor invariant contributions mentioned above.

The lower panel of Fig. 3 shows $|R^{(5)}_{xxzzxx}(t_1,t_2)|^2$ using the MBP model with the instantaneous normal mode (INM) vibrational DOS for xenon appearing in the inset [22]. The presence of an echo signal for the $R^{(5)}_{xxzzxx}$ polarization condition was suggested by Fourkas *et al.* and only appears using the MBP model [18]. The use of the FODID approximation acts to remove distinguishing contributions to differing polarization conditions by only allowing the triple product invariant to contribute with varying magnitudes [12,18]. The echo peak implies that an intermolecular mode, excited at time zero, is still oscillating at the time of the echo. As shown in Fig. 3, associating a period with the oscillation leads to the first echo signature at 53 cm^{-1} (100 fs) and the end of the signal occurs at a frequency of 12 cm^{-1} (450 fs). The echo onset frequency is in the tail of the INM DOS and the last echo occurs near the maximum of the INM DOS and the echo signature spans nearly the entire INM DOS. The appearance of an echo in such a simple liquid implies that intermolecular modes may generally live at least a period in more complicated liquids that have significant Lennard-Jones interactions.

Given the present computationally tractable theory for $R^{(5)}(t_1,t_2)$, examining the temperature dependence of the signal for liquid xenon and for other liquids and solutions will help establish the nature of the fifth-order Raman measurement and its variability—deeply supercooled liquids might be especially interesting considering the onset of nearly harmonic dynamics in that regime. Using the current theory to examine other polarizations will provide further insights into the information content of fifth-order Raman responses of molecular liquids. TCF theories bring the power of MD simulations to bear on the difficult task of theoretically modeling the spectroscopy of complex condensed phase chemical systems. When multidimensional nonlinear optical experiments were first proposed it was expected they could have an impact similar to introducing higher-dimensional techniques into NMR. A major impediment to developing and interpreting these spectroscopies has been the lack of a tractable yet accurate molecularly detailed theory of the spectroscopy and TCF theories serve to fill this void. Lastly, further work is needed to explain the absence of echo features in the molecular liquids studied to date.

The research was supported by NSF Grants No. CHE-0312834 (B. S.) and No. CHE-0352026 (T. K.), and a grant from ACS/PRF (B. S.). Finally, the authors are grateful for the use of data from earlier work by Richard Stratt and Ao Ma.

[1] Y. Tanimura and S. Mukamel, J. Chem. Phys. **99**, 9496 (1993).
[2] K. Kubarych, C. Milne, S. Lin, V. Astinov, and R. Miller, J. Chem. Phys. **116**, 2016 (2002).
[3] V. Astinov, K. Kubarych, C. Milne, and R. D. Miller, Chem. Phys. Lett. **327**, 334 (2000).
[4] O. Golonzka, N. Demirdoven, M. Khalil, and A. Tokmakoff, J. Chem. Phys. **113**, 9893 (2000).
[5] K. Okumura, A. Tokmakoff, and Y. Tanimura, J. Chem. Phys. **111**, 492 (1999).
[6] L. J. Kaufman, J. Heo, L. D. Ziegler, and G. R. Fleming, Phys. Rev. Lett. **88**, 207402(R) (2002).
[7] J. Kim and T. Keyes, Phys. Rev. E **65**, 061102 1 (2002).
[8] R. L. Murry, J. T. Fourkas, and T. Keyes, J. Chem. Phys. **109**, 2814 (1999).
[9] T. I. Jansen, K. Duppen, and J. Snijders, Phys. Rev. B **67**, 134206 (2003).
[10] R. A. Denny and D. R. Reichman, Phys. Rev. E **63**, 065101(R) (2001).
[11] A. Ma and R. M. Stratt, Phys. Rev. Lett. **85**, 1004 (2000).
[12] A. Ma and R. M. Stratt, J. Chem. Phys. **116**, 4962 (2002).
[13] S. Mukamel, *Principles of Nonlinear Optical Spectroscopy* (Oxford University Press, Oxford, 1995).
[14] J. Cao, S. Yang, and J. Wu, J. Chem. Phys. **116**, 3760 (2002).
[15] S. Mukamel, V. Khidekel, and V. Chernyak, Phys. Rev. E **53**, R1 (1996).
[16] R. DeVane, C. Ridley, T. Keyes, and B. Space, J. Chem. Phys. **119**, 6073 (2003).
[17] S. Saito and I. Ohmine, Phys. Rev. Lett. **88**, 207401 (2002).
[18] R. L. Murry and J. T. Fourkas, J. Chem. Phys. **107**, 9726 (1997).
[19] N.-H. Ge, M. T. Zanni, and R. M. Hochstrasser, J. Phys. Chem. A **106**, 962 (2002).
[20] J. Borysow, M. Moraldi, and L. Frommhold, Mol. Phys. **56**, 913 (1985).
[21] K. Okumura and Y. Tanimura, J. Chem. Phys. **107**, 2267 (1997).
[22] The INM DOS was calculated drawing 1000 statistically independent configurations of 108 Lennard-Jones particles from microcanonical MD. Using the configurations, the systems force constant matrix was calculated and diagonalized. The imaginary frequencies are shown on the negative abscissa.